

***In situ* x-ray scattering study of Ag(110) nanostructuring by ion erosion**C. Boragno, F. Buatier de Mongeot, G. Costantini, and U. Valbusa  
*INFM-UdR Genova and Dipartimento di Fisica, Genova, Italy*R. Felici  
*OGG INFM, c/o ESRF, Grenoble, France*D.-M. Smilgies  
*CHESS, Cornell University, Ithaca, New York 14853*S. Ferrer  
*ESRF, Grenoble, France*

(Received 25 September 2001; published 29 March 2002)

The time evolution of the morphology of the Ag(110) surface during ion sputtering has been studied *in situ* and in real time by x-ray based techniques. The surface was bombarded with Ar<sup>+</sup> ions at an energy of 1 keV in the temperature range 100–320 K. Grazing-incidence x-ray scattering measurements have been carried out in order to characterize the shape and the time evolution of the regular structures (mounds or ripples) created on the surface. The results show that the periodicity (i.e., the average separation between features) increases as function of the sputtering time, following a power-law behavior. Moreover, the slope of the mounds/ripples depends on temperature, ranging between 6 and 12° if measured along the  $\langle 1 - 1 0 \rangle$  direction and between 8 and 10° along  $\langle 0 0 1 \rangle$ .

DOI: 10.1103/PhysRevB.65.153406

PACS number(s): 68.55.Jk, 68.37.-d, 61.10.-i

Ion sputtering is an important process for the removal of material from surfaces through the impact of energetic particles. Detailed understanding of this erosion process is of great interest, because it is commonly used in analytical techniques for surface cleaning or depth profiling. It can also be used to improve the quality of thin films when it is used in combination with molecular-beam epitaxy.<sup>1</sup> Recently, it has also been shown that sputtering can be used for nanopatterning of surfaces.<sup>2</sup> Ripple pattern formation has been observed in oxides and semiconductors when the surfaces are bombarded with 1-keV Xe<sup>+</sup> ions.<sup>3–5</sup> In these cases the structures are interpreted as interface instabilities caused by sputtering erosion which competes with slow surface diffusion. In the case of metals, surface atomic diffusion biased by Ehrlich-Schwoebel barriers might become the leading process responsible for the structure formation. Pits of hexagonal shape appear in isotropic surfaces as Pt(111) (Ref. 6) or Au(111),<sup>7</sup> and square holes have been observed in Ag(001) (Ref. 8) and Cu(001).<sup>9,10</sup> In the case of anisotropic surfaces, the asymmetry induces a self-aggregation at the surface leading to the formation of characteristic ripplelike structures.<sup>11</sup> Due to the different activation energies for surface diffusion along or perpendicular to the easy direction, which for a  $\langle 1 1 0 \rangle$  surface is parallel to the  $\langle 1 - 1 0 \rangle$  direction, the structure of the ripple orientation strongly depends either on the sputtering angle or on the surface temperature.<sup>12,13</sup>

The majority of these experiments have been done by scanning tunnel microscopy (STM), a method which, however, does not allow us to follow the evolution of the morphology *in real time*. X-ray diffraction overcomes this limitation, since data can be taken during the ion etching process.<sup>7,14</sup> In order to exploit the capabilities of the x-ray techniques, we measured the time dependence of the forward

scattering using grazing incidence small-angle scattering (GISAXS). The sample was further characterized in the late stages of sputtering by the measurement of the crystal truncation rods (CTR's) for the two inequivalent high-symmetry directions. GISAXS spectra provide information on the correlation of surface density fluctuations and thus about the long-range morphological order.<sup>15</sup> CTR's are due to the truncation of the lattice induced by the surface. In a surface consisting of microfacets, each of them has an associated diffraction rod directed along the normal of the facet plane. By measuring the diffracted intensity along these directions in reciprocal space it is possible to determine the orientation of the microfacets in the crystal surface with high accuracy.<sup>16</sup> In this paper we report on our studies about the morphology evolution of Ag(110) during 1-keV Ar<sup>+</sup> sputtering. Under similar conditions of surface temperature and sputter flux, this system presents a transition from a rough to a smooth surface, passing through the formation of ordered structures, by increasing the sample temperature.<sup>8</sup>

Measurements were carried out at the ID03 beamline of the European Synchrotron Radiation Facility in Grenoble, France. This beamline is devoted to surface x-ray-diffraction measurements and is equipped with a large six-circle diffractometer coupled to a UHV chamber with a base pressure of about 10<sup>-10</sup> mbar.<sup>17</sup> The sample holder is connected to a liquid-nitrogen flow cryostat to cool the sample down to a minimum temperature of 120 K. The sample was mounted on a boron nitride heater and the temperature was controlled by a thermocouple in contact with the sample. The accuracy on the sample temperature is ±5 K. The Ag(110) surface had a miscut from the nominal surface of less 0.1°. The surface was prepared by several cycles of sputtering and annealing at 750 K for 5 min, repeating the procedure every time before

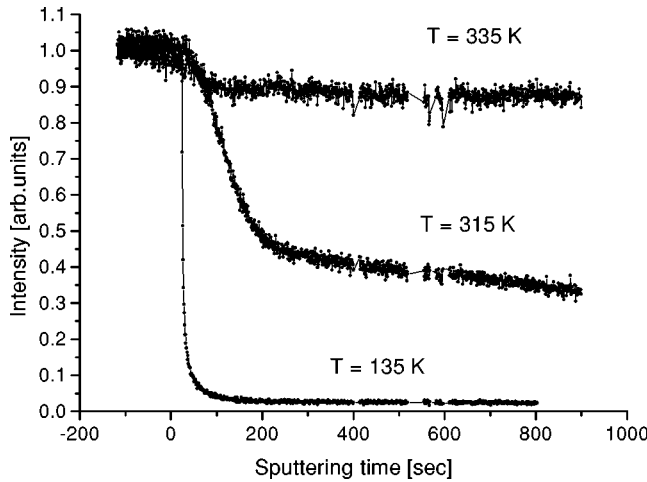


FIG. 1. Evolution of the CTR intensity at the (1 0 0.6) position during  $\text{Ar}^+$  irradiation at three different temperatures.

each sputtering experiment. The  $\text{Ar}^+$  ion sputtering was performed using a Varian ion gun and controller at a constant current of  $8 \mu\text{A}/\text{cm}^2$ , corresponding to an ion flux of about 0.056 monolayer/sec (ML/sec [1 ML =  $8.44 \times 10^{14}$  atom/ $\text{cm}^2$  for Ag(110)]). The angle of incidence of the ion beam was about  $16^\circ$  with respect to the surface normal.

The Ag(110) surface is anisotropic in nature: close-packed rows of atoms run along  $\langle 1 -1 0 \rangle$ , whereas in the  $\langle 0 0 1 \rangle$  direction the interatomic distance is  $\sqrt{2}$  times the nearest-neighbor distances. The surface unit cell is given by  $A_1$ ,  $A_2$ ,  $A_3$  which are parallel to the  $\langle 1 -1 0 \rangle$ ,  $\langle 0 0 1 \rangle$ , and  $\langle 1 1 0 \rangle$  directions, respectively, with  $A_1 = A_3 = 0.2891$  nm, and  $A_2 = 0.4089$  nm. The corresponding reciprocal-lattice directions are designed as  $H$ ,  $K$ ,  $L$ , respectively. Bulk Bragg reflections based on this lattice are found at  $(H, K, L)$  values with  $L = 0, 2, 4, \dots$  or  $L = 1, 3, 5, \dots$ , depending on whether  $H$  and  $K$  have the same or different parity. As is customary in surface x-ray diffraction, the  $L$  values denote the perpendicular momentum transfer and are continuously varying along the so-called crystal truncation rods.

In Fig. 1 we report the temporal evolution of the diffracted intensity at (1, 0, 0.6) while the surface was being sputtered for three different temperatures. At this CTR position we are close to out-of-phase conditions, maximizing sensitivity to changes in the surface roughness.<sup>14</sup> These curves are representative of a large series of spectra acquired in the temperature range 130–335 K. The nearly constant decay at 335 K is a clear indication that the surface evolves via step retraction. Below this temperature the intensity decays fast with sputter time indicating the development of three-dimensional roughness. We did not detect intensity oscillations typical of layer-by-layer erosion, as was observed for similar systems.<sup>18–21</sup> In Fig. 2(a) we show GISAXS spectra taken at 195 K. The spectra show the variation of the specular beam intensity at the (0 0 0.06) reciprocal-lattice point along the  $H$  direction. The incident x-ray beam is parallel to the  $\langle 0 0 1 \rangle$  (surface azimuth angle =  $0^\circ$ ). The spectra were collected continuously during sputtering with an acquisition time for a single scan of about 100 sec. Two side peaks

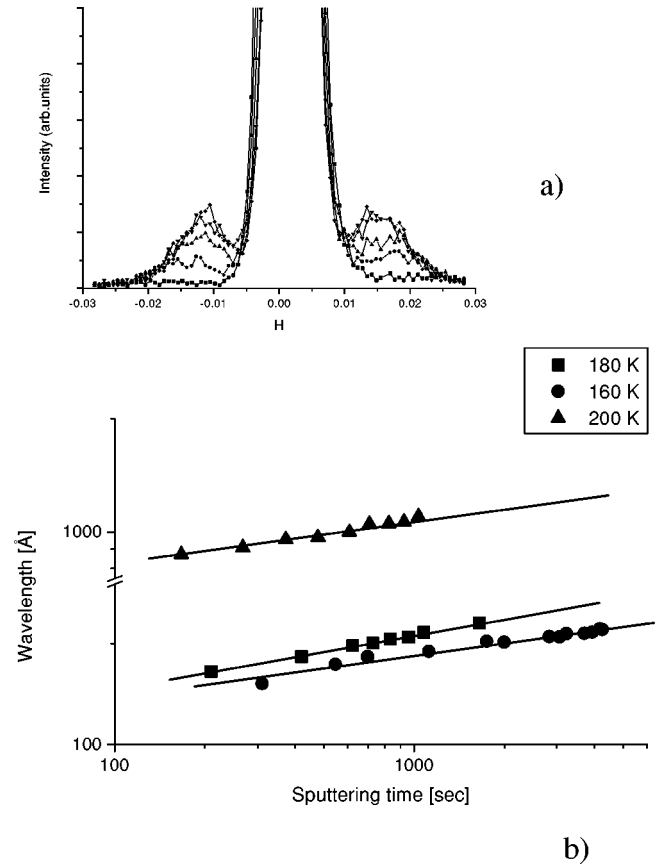


FIG. 2. GISAXS scans at the (0 0 0.6) position at a surface temperature  $T = 195$  K. From bottom to top, the spectra have been acquired after 0, 900, 2000, 3400, and 4600 sec of sputtering, respectively. (b) scaling law of the wavelength vs sputtering at three different temperatures.

are present which move towards the specular peak with sputtering time. At this temperature the satellite peaks are not observable when the azimuthal angle of the sample is rotated by  $90^\circ$  (i.e., incident wave vector parallel to  $\langle 1 -1 0 \rangle$ ). Since it is well known that for transverse scans at low vertical momentum, the observation of satellite peaks can be unambiguously associated to the average distance between surface features,<sup>22</sup> the present observation indicates the formation of ripples along the  $\langle 0 0 1 \rangle$  direction whose wavelength evolves in time. From the position of the two peaks, it is possible to calculate the ripple period  $\lambda = 2\pi/q_p$  where  $q_p$  is the distance of the center of the satellite from the diffraction peak. The result of this analysis is shown in Fig. 2(b) for three different temperatures. The log-log plot reveals a clear power-law behavior with an exponent equal to  $0.16 \pm 0.01$  at  $T = 215$  K,  $0.13 \pm 0.01$  at  $T = 195$  K, and  $0.13 \pm 0.01$  at 245 K.

In Fig. 3(a) we show rocking scans of the (1 0  $L$ ) CTR for various  $L$  values around the Bragg reflection at  $L = 1$ . These scans acquired at 265 K at a late stage of the sputtering process clearly show a split rod indicative of faceting of the surface. By plotting the observed  $H$  values of the peaks versus  $L$ , we determined the local slope of the facets, in this case equal to  $10^\circ \pm 1^\circ$  [Fig. 3(b)]. For all temperatures studied in the range of 130–310 K, CTR scans were acquired after

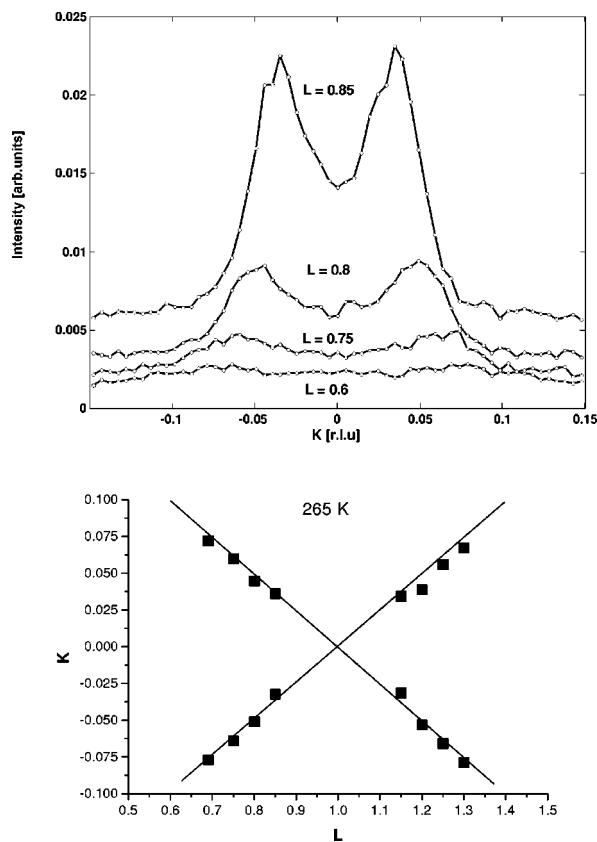


FIG. 3. (a) CTR rocking scans acquired at the  $(1\ 0\ L)$  position at  $T = 265$  K, for various  $L$  values, as indicated. The splitting of the CTR is a signature of the faceted surface at the late stage of sputtering. (b) Plot of the peak positions as function of  $L$  revealing the average slopes of the facets.

about 1 h of sputtering with the sputter gun still on. We observed on a similar system that after this time the surface dynamics slows down and the slope reaches a quasiconstant value.<sup>23</sup> At  $T = 135$  K, only the  $H$  scans show well defined satellites, indicating that the surface is periodically corrugated only along  $\langle 001 \rangle$ , in agreement with the GISAXS measurements.

Increasing the temperature results in the appearance of satellites of the  $(1,0,L)$  rod along the  $H$  and  $K$  directions, indicating that the surface is arranged in rectangular mounds, whose slopes depend on  $T$  and on the surface azimuth. In Fig. 4, we plot the average slope along the two principal surface directions at various temperatures. The two curves show maxima of  $12^\circ$  at  $T = 215$  K along  $\langle 0\ 0\ 1 \rangle$  and about  $10^\circ$  at  $T = 265$  K along  $\langle 1\ -1\ 0 \rangle$ .

The results reported above show that the Ag(110) surface assumes different regular morphologies, from ripples to regular mounds, if bombarded with energetic ions. The observed behavior is consistent with recent STM results, however, avoiding possible inaccuracies associated with the temperature quenches used in the STM experiments. The data reported in Fig. 1 indicate that the erosion, in our case, is never layer by layer, but proceeds via step retraction at high temperatures and via the development of three-

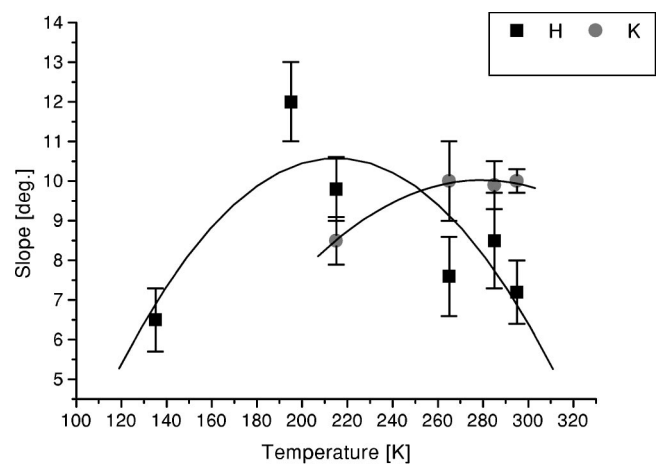


FIG. 4. Facet slopes vs temperature, as determined from CTR scans in both the  $H$  and  $K$  directions, like the ones shown in Fig. 3. The continuous lines are guides to the eye.

dimensional roughness at low temperatures.

At all studied temperatures, the GISAXS measurements show a time evolution of the wavelength which can be described with a power law.<sup>24</sup> The experimental values of the exponent  $z$  are in the range 0.13–0.16 and substantially do not depend on the surface temperature or on the crystallographic direction. The observed values are smaller than those observed in similar experiments on Cu(110) (Ref. 13) and Au(111),<sup>18</sup> where  $z$  is around 0.25, a value predicted in a continuum model by Siegert and Plischke<sup>25</sup> for epitaxial deposition. The observed scaling behavior is different from the prediction from the Bradley and Harper model<sup>26</sup> for which there is no coarsening in the evolution of the ripple's wavelength.

From the CTR measurements we extracted the slope of the ripples and mounds at a late stage of the sputtering process. At low  $T$  (135 K), the ripple has a slope of  $5^\circ$  which roughly corresponds to an average terrace size of five atomic rows along  $\langle 0\ 0\ 1 \rangle$  which becomes  $12^\circ$  at 195 K, the maximum temperature for which the ripple is well defined. Above 210 K, the morphology changes to a mound structure: CTR scans along both  $H$  and  $K$  display well resolved satellites. However, the slope is different in the two high-symmetry directions: along  $\langle 0\ 0\ 1 \rangle$  the slope decreases from 10 to  $7^\circ$  while along  $\langle 1\ -1\ 0 \rangle$  it increases from 8 to  $10^\circ$ . This behavior can be easily interpreted as the onset of the ripple rotation, which sets in this temperature range<sup>11</sup> and it is fully developed at a temperature of 350 K. The latter regime was not explored in this experiment, because the large period of these ripples was beyond our present instrumental resolution.

In conclusion, we have been able to follow the evolution of the morphology of the Ag(110) surface *in situ* and in real time during 1-keV  $\text{Ar}^+$  bombardment and at various surface temperatures by exploiting x-ray scattering. By combining GISAXS and CTR information, we determined the time evolution of the average separation between surface features as well as the average surface slope at late stages of the sputter erosion process.

- <sup>1</sup>C. H. Choi, R. Ai, and S. A. Barnett, *Phys. Rev. Lett.* **67**, 2826 (1991).
- <sup>2</sup>S. Facsko, T. Dekorsy, C. Koerdt, C. Trappe, H. Kurz, A. Vogt, and H. L. Hartnagel, *Science* **285**, 1551 (1999).
- <sup>3</sup>E. Chason, T. M. Mayer, B. K. Kellerman, D. T. McIlroy, and A. J. Howard, *Phys. Rev. Lett.* **72**, 3040 (1994).
- <sup>4</sup>S. Jay Chey, J. E. Van Nostrand, and D. G. Cahill, *Phys. Rev. B* **52**, 16 696 (1995).
- <sup>5</sup>J. Erlebacher, M. J. Aziz, E. Chason, M. B. Sinclair, and J. A. Floro, *Phys. Rev. Lett.* **82**, 2330 (1999).
- <sup>6</sup>T. Michely and G. Comsa, *Nucl. Instrum. Methods Phys. Res. B* **82**, 207 (1993).
- <sup>7</sup>R. M. V. Murty, T. Curcic, A. Judy, B. H. Cooper, A. R. Woll, J. D. Brock, S. Kycia, and R. L. Headrick, *Phys. Rev. Lett.* **80**, 4713 (1998).
- <sup>8</sup>S. Rusponi, G. Costantini, F. B. de Mongeot, C. Boragno, and U. Valbusa, *Appl. Phys. Lett.* **75**, 3318 (1999).
- <sup>9</sup>M. Ritter, M. Stindtmann, M. Farle, and K. Baberschke, *Surf. Sci.* **348**, 243 (1996).
- <sup>10</sup>H. J. Ernst, *Surf. Sci.* **383**, L755 (1997).
- <sup>11</sup>S. Rusponi, C. Boragno, and U. Valbusa, *Phys. Rev. Lett.* **78**, 2795 (1997).
- <sup>12</sup>S. Rusponi, G. Costantini, C. Boragno, and U. Valbusa, *Phys. Rev. Lett.* **81**, 2735 (1998).
- <sup>13</sup>S. Rusponi, G. Costantini, C. Boragno, and U. Valbusa, *Phys. Rev. Lett.* **81**, 4184 (1998).
- <sup>14</sup>D. M. Smilgies, P. J. Eng, E. Landemark, and M. Nielsen, *Surf. Sci.* **377–379**, 1038 (1997).
- <sup>15</sup>M. Rauscher, R. Paniago, H. Metzger, Z. Kovats, J. Domke, J. Peisl, H. D. Pfannes, J. Schulze, and I. Eisele, *J. Appl. Phys.* **86**, 6763 (1999).
- <sup>16</sup>I. K. Robinson and D. J. Tweet, *Rep. Prog. Phys.* **55**, 599 (1992).
- <sup>17</sup>S. Ferrer and F. Comin, *Rev. Sci. Instrum.* **66**, 1674 (1995).
- <sup>18</sup>M. V. Ramana Murty, T. Curcic, A. Judy, B. H. Cooper, A. R. Woll, J. D. Brock, S. Kycia, and R. L. Headrick, *Phys. Rev. B* **60**, 16 956 (1999).
- <sup>19</sup>P. Bedrossian, J. E. Houston, J. Y. Tsao, E. Chason, and S. T. Picraux, *Phys. Rev. Lett.* **67**, 124 (1991).
- <sup>20</sup>B. Poelsema, L. K. Verheij, and G. Comsa, *Phys. Rev. Lett.* **53**, 2500 (1991).
- <sup>21</sup>P. Bedrossian and T. Klitsner, *Phys. Rev. B* **44**, 13 783 (1991).
- <sup>22</sup>H. You, K. G. Huang, and R. T. Kampwirth, *Physica B* **221**, 77 (1996).
- <sup>23</sup>C. Boragno, F. Buatier de Mongeot, G. Costantini, U. Valbusa, R. Felici, and S. Ferrer (unpublished).
- <sup>24</sup>J. G. Amar and F. Family, *Phys. Rev. B* **54**, 14 742 (1996).
- <sup>25</sup>M. Siegert and M. Plischke, *Phys. Rev. Lett.* **73**, 1517 (1994).
- <sup>26</sup>R. M. Bradley and J. M. E. Harper, *J. Vac. Sci. Technol. A* **6**, 2390 (1988).